Agriculture & Food Security

RESEARCH Open Access

Green synthesis, characterization, antibacterial and photocatalytic activity of black cupric oxide nanoparticles

Khwaja Salahuddin Siddiqi[1], M. Rashid[2], A. Rahman[2], Tajuddin[2], Azamal Husen[3*] and Sumbul Rehman[4]

Abstract

Background: Biogenic fabrication of nanoparticles from naturally occurring biomaterials involves plants, herbs, bacteria and fungi using water as neutral solvent, while chemical synthesis involves hazardous chemicals and leaves unwanted byproduct which unnecessarily pollute the environment. In order to prevent atmospheric pollution a safe, clean and green strategy for the synthesis of cupric oxide nanoparticles from aqueous leaf extract of *Diospyros montana* has been employed. *D. montana* of Ebenaceae family is a poisonous tropical plant which grows wild in Asia. Its extract is commonly known as fish poison. The rate of formation of NPs from plant extract is thought to be facile and rapid relative to those formed by fungi and bacteria, but it depends on the concentration of reducing chemicals available in the extract. We report, in this communication, a benign method of biogenic synthesis of cupric oxide nanoparticles (CuO-NPs) from leaf extract of *D. montana* and their characterization by UV–visible, FTIR, SEM, TEM, DLS, SAED and EDX analyses. Their antimicrobial activity against seven Gram-positive and four Gram-negative bacteria has been screened. Photocatalytic degradation of methylene blue by ascorbic acid as reducing agent and cupric oxide nanoparticles as catalyst has been done under sunlight.

Results: Cupric oxide nanoparticles of varying size starting from 5.9 to 21.8 nm have been fabricated from aqueous leaf extract of *D. montana* at room temperature. The pure extract absorbs at 273 nm while CuO-NPs exhibit a broad peak at 320 nm. FTIR spectrum of the leaf extract shows the presence of a double quinonoid molecule. There are three types of CuO-NPs with different hydrodynamic radii. Their average hydrodynamic radii fall between 495 ± 346 nm. SEM and TEM images show spherical shaped CuO-NPs of different size. SAED suggests crystalline nature of CuO-NPs. They are highly polydispersed in solution. EDX analysis reveals the presence of Ca, C, O, Na and Si besides copper. Oxygen content is over 50% by mass. Reduction of methylene blue dye (MB) by ascorbic acid as reducing agent, in presence of CuO-NPs as catalyst, has been achieved in 90 s at room temperature while their reduction by ascorbic acid alone takes more than 10 min. Antibacterial activity of CuO-NPs against seven Gram-positive (*Staphylococcus aureus, Streptococcus mutans, Streptococcus pyogenes, Streptococcus viridans, Staphylococcus epidermidis, Corynebacterium xerosis and Bacillus cereus*) and four Gram-negative bacterial strains (*Escherichia coli, Klebsiella pneumoniae, Pseudomonas aeruginosa* and *Proteus vulgaris*) has been investigated. The results indicated that NPs are highly effective against growth inhibition of Gram-positive bacteria than Gram-negative bacteria. Copper oxide nanoparticles are even more toxic than the standard antibiotic, norfloxacin.

Conclusion: In this project cupric oxide NPs of 5.9–21.8 nm have been fabricated from aqueous leaf extract of *D. montana*. It is most inexpensive and easy process to fabricate NPs from plant material because no toxic chemicals are

*Correspondence: adroot92@yahoo.co.in
[3] Wolaita Sodo University, P.O. Box: 138, Wolaita, Ethiopia
Full list of author information is available at the end of the article

used. Since CuO-NPs are toxic to several Gram-positive and Gram-negative bacterial strains, attempt may be made to use them as antibacterial agent to protect food, vegetable and crops. Also, the reduction of methylene blue dye by ascorbic acid as reducing agent in presence of CuO NPs as catalyst has been done very efficiently at a rapid rate which prompts us to use them as catalyst in the reduction of dyes, other toxic materials and industrial effluents. Further investigation of other beneficial properties of CuO-NPs can also be explored.

Keywords: Green synthesis, *Diospyros montana*, Electron microscopy, Antibacterial activities, Catalytic property

Introduction

Copper (Cu) is one of the coinage metals known to human beings since metallic age. Of the two common oxidation states of copper, Cu^{2+} is more stable both as salt or complex. It is a good conductor of heat and electricity. When copper metal is exposed to moist air it forms a green protective layer of basic copper sulfate. It is also used in alloys like brass and bronze. Since copper is also required in human being to activate certain enzymes people use copper vessels to store drinking water. Copper is an essential constituent of several enzymes such as super oxide dismutase and ceruloplasmin without which the enzymes lose their activity.

Cupric oxide (CuO) is black while cuprous oxide (Cu_2O) is red. It is slowly oxidized to black cupric oxide when exposed to air. Metallic copper is shining dull red in pure state and so is the color of copper nanoparticles (Cu-NPs). Cu-NPs of approximately 5 nm generally do not show any absorption peak in UV–Vis region [1–3]. However, a mixture of small and large NPs exhibit a peak between 560–570 nm and even below 350 nm depending on the ratio of their size in the colloidal mixture [3, 4].

Green route of fabrication of NPs from natural sources involves plants, herbs, bacteria and fungi using water as neutral solvent [5–8]. The rate of formation of NPs from plant extract is faster relative to those synthesized by fungi and bacteria but it all depends on the concentration of reducing chemicals available in the extract [9–12]. Cupric oxide nanoparticles are frequently fabricated to study their multifunctional application in biosensor, electronics, photocatalytic degradation of dyes and chemical industry. Sankar et al. [12] have reported the catalytic activity of CuO-NPs biosynthesized from *Carica papaya* leaf extract. The degradation of Coomassie brilliant blue dye R-250 using CuO as catalyst has been achieved in sunlight. A decrease in absorption intensity of the dye in presence of CuO-NPs after about 2 h has been taken as an evidence of its degradation without undergoing any change in original absorption at 559 nm in the visible region of spectrum. The dye degradation has been attributed to the size and morphology of CuO-NPs. However, in a mixture containing various types of NPs a specific type of NPs cannot be held responsible for effective degradation of dye until selected NPs of known size are used in the experiment [13, 14].

Copper sulfate is the major constituent of Bordeaux mixture ($CuSO_4$ 1 kg, quick lime 1 kg, water 100 L), which is used as biocide in protecting crops from insects and microbes [15]. Copper and CuO-NPs are known for their use in biological system as they usually inhibit the growth of pathogenic microorganisms and algae [16–18]. Cupric oxide, also known as calx is used in medicine. It is recommended for local application in skin diseases in the oriental system of medicine [19].

Biogenic synthesis of CuO-NPs from aqueous extract of *Gundelia tournefortii* and their application as catalyst has been evaluated [20]. They have been used in the synthesis of naturally occurring urea and in the reduction of 4-nitrophenol to 4-amino phenol. The aqueous alcoholic extract of *G. tournefortii* is known to contain phenolic compounds, particularly caffeic acid derivatives which are antioxidant and act as reducing and stabilizing agent [21, 22]. Cupric ion is suggested to be first reduced to copper metal and subsequently oxidized to CuO-NPs when heated in open.

$$Cu^{2+} + 2\bar{e} \rightarrow Cu^0$$

$$Cu^0 \rightarrow CuO + 2\bar{e}$$

Nagajyothi et al. [23] have proposed that the precursor $CuSO_4.5H_2O$ first reacts with OH ions produced by water molecules giving $Cu(OH)_2$ which subsequently interacts with phytochemicals present in the plant extract leading to the formation of CuO-NPs. It is practically not possible that water will produce OH^- ions without any initiation and will subsequently react with $CuSO_4$. Had it been true, $CuSO_4$ would have produced bluish white precipitate of $Cu(OH)_2$, which is not the case. However, $Cu(OH)_2$ is produced only when the copper sulfate is made alkaline by adding sodium hydroxide which will produce CuO on heating, as shown below.

$$CuSO_4 + 2NaOH \rightarrow Cu(OH)_2 + Na_2SO_4$$

$$Cu(OH)_2 \rightarrow CuO + H_2O$$

Hydration of phenylcyanamide to urea by CuO-NPs and acetaldoxime has been facilitated [24]. Maximum yield was obtained at 10.0 mol% of CuO. Its efficiency was found to be much greater than those obtained by known catalysts such as $ZrCl_4$ and BF_3. Reduction of 4-nitrophenol to 4-aminophenol in presence of KBH_4 and CuO-NP has also been achieved. Complete reduction was done in 70 s at a concentration of 10 mg CuO-NP which was monitored by UV–Vis spectrum of the substrate. Since the CuO-NP is a heterogeneous catalyst, it is easily separated and recycled without losing its activity.

Aqueous extract of *Anthemis nobilis* flowers has been exploited for the synthesis of CuO-NPs [25]. The extract contains phenolic compounds which are responsible for the production of CuO-NPs [26]. They are highly stable and crystalline with face centered cubic (fcc) structure. The CuO-NPs were catalytically effective for the synthesis of propargylamines. Synthesis of Pd/CuO-NPs from *Theobroma cacao* seed extract has been reported [27]. They have been used in the reduction of 4-nitrophenol to 4-aminophenol and, also in phosphine-free Heck coupling reaction. This reaction is particularly employed in the synthesis of biologically active molecules where Pd/CuO-NPs are used as heterogeneous catalysts. Reduction of 4-nitrophenol to 4-amino phenol by $NaBH_4$ as a reducing agent and Pd/CuO-NPs as catalyst occurs with the formation of nitrophenolate ion as an intermediate. It follows the first-order kinetics.

Diospyros montana belonging to Ebenaceae family is a poisonous tropical plant. It has been reported that its aqueous extract contains betulin, diospyrin, mamegakinone, oleanolic acid and lupiol [28]. Diospyrin, a biquinone is the major constituent of the extract which interacts with the metal ions to produce metal/metal oxide NPs [29]. In view of the miscellaneous properties, we have undertaken the green route of synthesis of cupric oxide NPs using aqueous leaf extract of *D. montana* and $CuSO_4$. Their characterization by HPLC, UV–Vis, FTIR spectroscopy, SEM, TEM, SAED, DLS and EDX analysis has been done. Antimicrobial activity of CuO-NPs against both Gram-positive and Gram-negative bacterial strains has been evaluated to see if they may be used to inhibit the growth of pathogenic microbes. Photocatalytic degradation activity of these NPs against methylene blue dye using ascorbic acid as reducing agent has also been carried out.

Materials and methods

Plant materials and synthesis of CuO-NPs

Leaf extract of *D. montana* was prepared by taking 10 g dried leaf powder in 100 ml distilled water. It was stirred for 5 h at room temperature and then filtered through a Whatman filter paper number 40. 10 ml of this greenish yellow extract at pH 6.8 was taken in an Erlenmeyer flask and 10 ml of 0.01 M aqueous solution of $CuSO_4$ was added to it with continuous stirring. This mixture yielded black CuO-NP after about 20 min which settled at the bottom of container. If this mixture is heated at about 60 °C, precipitation occurs within 5 min. The CuO-NP thus prepared was centrifuged at 3000 rpm with a REMI R-4C DX centrifuge machine and washed several times to remove excess of either of the reacting components. They were dried in an oven at 60–70 °C.

Characterization techniques

UV–Vis spectra were recorded with a Motras UV Plus double beam spectrophotometer working at a resolution of 1 nm. FTIR spectra were recorded with a Perkin Elmer spectrometer, Perkin Elmer Spectrum version 10.4.00 as KBr disc over the 500–4000 cm^{-1} region. Colloidal solution of biosynthesized CuO-NP was drop cast on a carbon-coated copper grid for TEM micrograph using JEOL, JEM2100 working at 200 kV. SEM analysis was done with a JEOL, JSM6510 LV instrument. Selected area electron diffraction (SAED) analysis was done on the same grid. Energy-dispersive X-ray analysis of (EDX) was carried out with an Oxford instrument Inca-model. Spectra were recorded in the spot profile mode by focusing electron beam onto a region on the surface coated with nanoparticles. Size distribution of nanoparticles was determined using MALVERN Dynamic Light Scattering (DLS) instrument with DLS version 6.20 at 25 °C at 357.8 derived count rate (K cps). Water was used as the solvent. The high-performance liquid chromatography (HPLC) profile of aqueous extract of the *D. montana* was generated by using a Shimadzu HPLC system equipped with a single pump and C18 column of 5 µm diameter (250×1.6 nm) filled with porous silica gel. The system consists of an LC 20 AD isocratic solvent pump, an UV/VIS SPD 20A detector and a rheodyne injector with position sensing switch and a 20 µl sample loop. Mobile phase consisted of HPLC-grade methanol. HPLC was run for 30 min at a flow rate of 1 ml/min. Results were obtained at 2 different wavelengths, i.e., 273 nm and 252 nm. The peaks eluted at different retention times were done. All determinations were performed at ambient temperature. Copper sulfate pentahydrate, $CuSO_4.5H_2O$ (SD fine chemicals) and HPLC-grade methanol (Merck India, Ltd.) were used without further purification. Double distilled water and sterilized glassware were used.

Photocatalytic degradation

The photocatalytic activity of the CuO-NPs was evaluated by employing methylene blue (MB) dye. Its reduction was carried out in a small bath and also in the open at room temperature. A 20 ppm aqueous solution of the

dye was prepared in a 100-ml standard flask. About 0.1 g solid ascorbic acid (CDH, India) as reducing agent, was added to 10 ml MB. 1–2 mg of CuO NPs was used as catalyst in each set of experiment. Three sets of experiment were done and the time taken to complete the degradation of MB was recorded.

In vitro antibacterial activity

Antibacterial activity of CuO-NPs was examined against seven Gram-positive (*Staphylococcus aureus, Streptococcus mutans, Streptococcus pyogenes, Streptococcus viridans, Staphylococcus epidermidis, Corynebacterium xerosis* and *Bacillus cereus*) and four Gram-negative bacterial strains (*Escherichia coli, Klebsiella pneumoniae, Pseudomonas aeruginosa* and *Proteus vulgaris*). The solid Nutrient Agar No. 2 (NA) (M 1269S-500G, Himedia Labs Pvt. Ltd, Bombay, India) was used for preparing nutrient plates, while Nutrient Broth (NB) (M002-500G, Himedia Labs Pvt. Ltd, Bombay, India) was used for liquid culture medium.

Antibacterial activity of cupric oxide NPs was evaluated by agar well diffusion method according to CLSI guidelines. All the microbial cultures were adjusted to 0.5 McFarland standards which is visually comparable to microbial suspension of 1.5×10^8 cfu/ml. Twenty ml of agar medium was poured into each petri plate and swabbed with a colony from the inoculums of the test microorganism and left for 15 min for absorption. Using sterile cork borer of 6 mm diameter, wells were bored into the seeded agar plates and were loaded with a 100 µl

Table 1 HPLC profile of aqueous leaf extract of *Diospyros montana* at 273 nm

Peak	Retention time	Area	Height	Area%	Height%
1	2.34	87,722.00	12,632.00	1.73	4.05
2	2.66	794,579.00	59,202.00	15.66	18.98
3	2.88	734,674.00	86,801.00	14.48	27.84
4	2.98	1,260,815.00	97,597.00	24.85	31.31
5	3.22	2,193,681.00	55,289.00	43.24	17.73
6	6.99	2136.00	244.00	0.042	0.08
Total		5,073,608.00	311,765.00	100.00	100.00

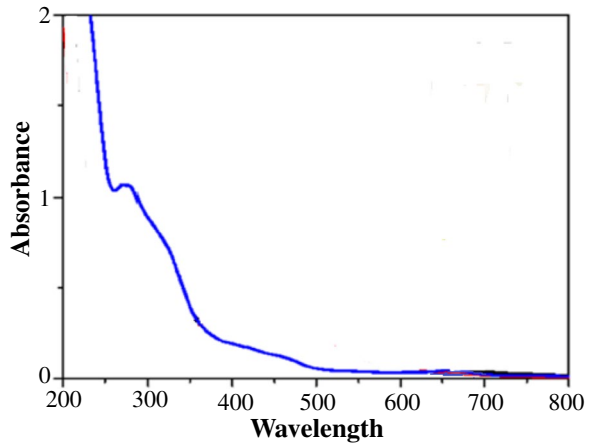

Fig. 2 UV–Vis spectrum of aqueous leaf extract of *Diospyros montana*

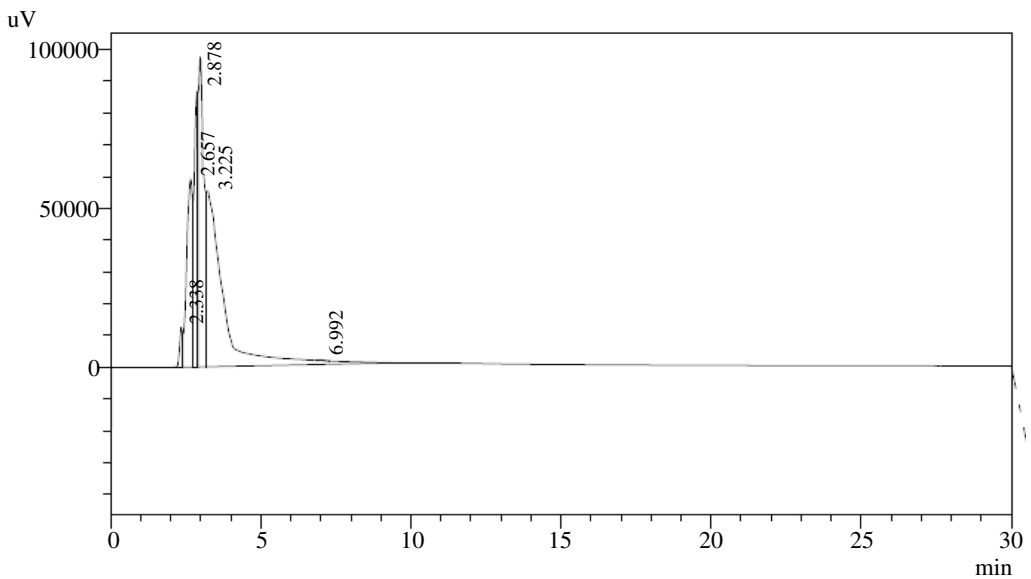

Fig. 1 HPLC profile of aqueous extract of *Diospyros montana* at 273 nm

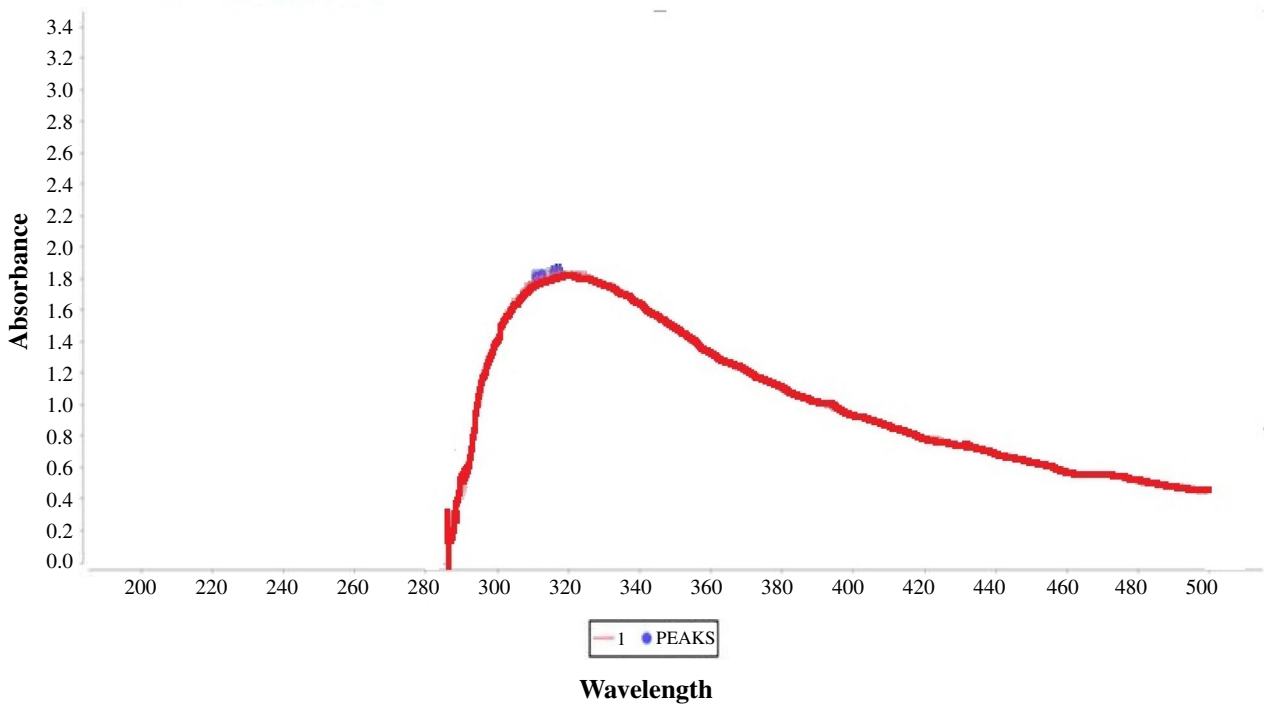

Fig. 3 UV–Vis spectrum of CuO-NPs fabricated from leaf extract of *Diospyros montana*

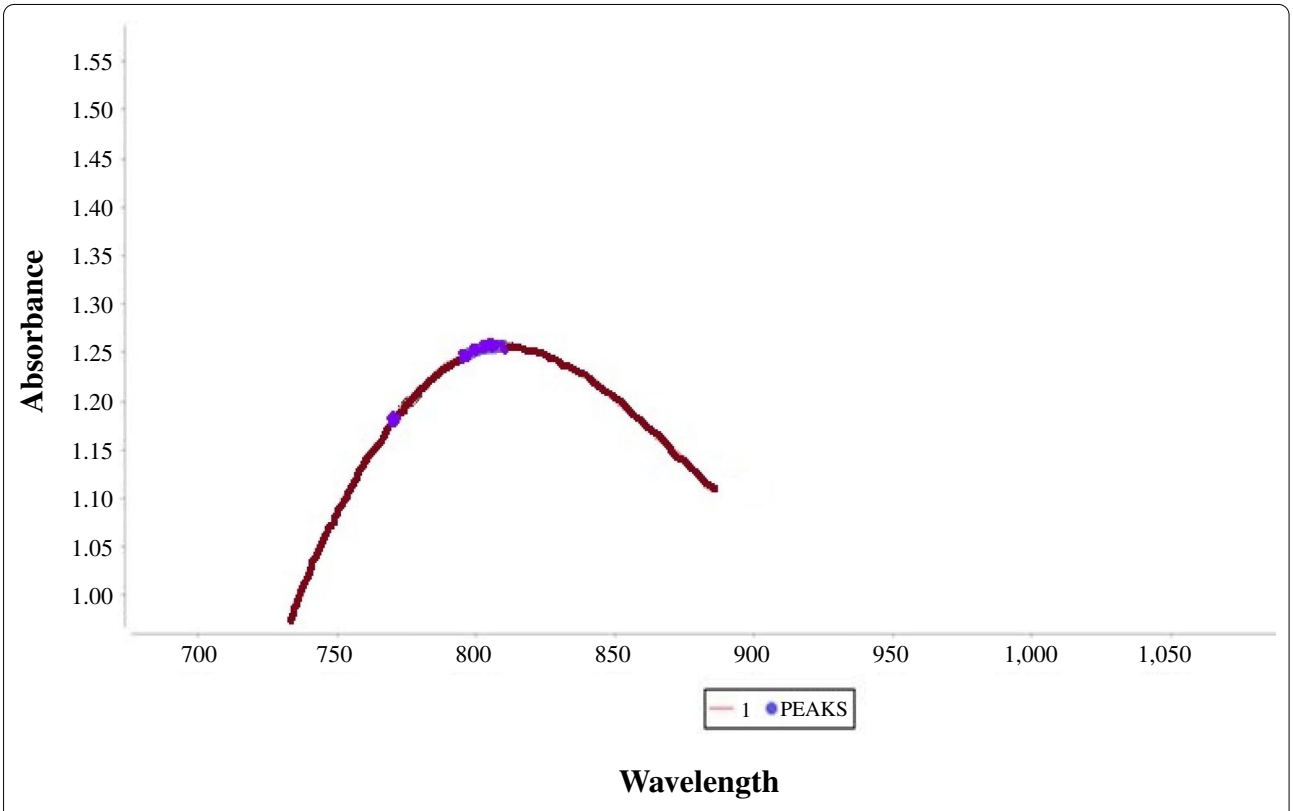

Fig. 4 UV–Vis spectrum of $CuSO_4$

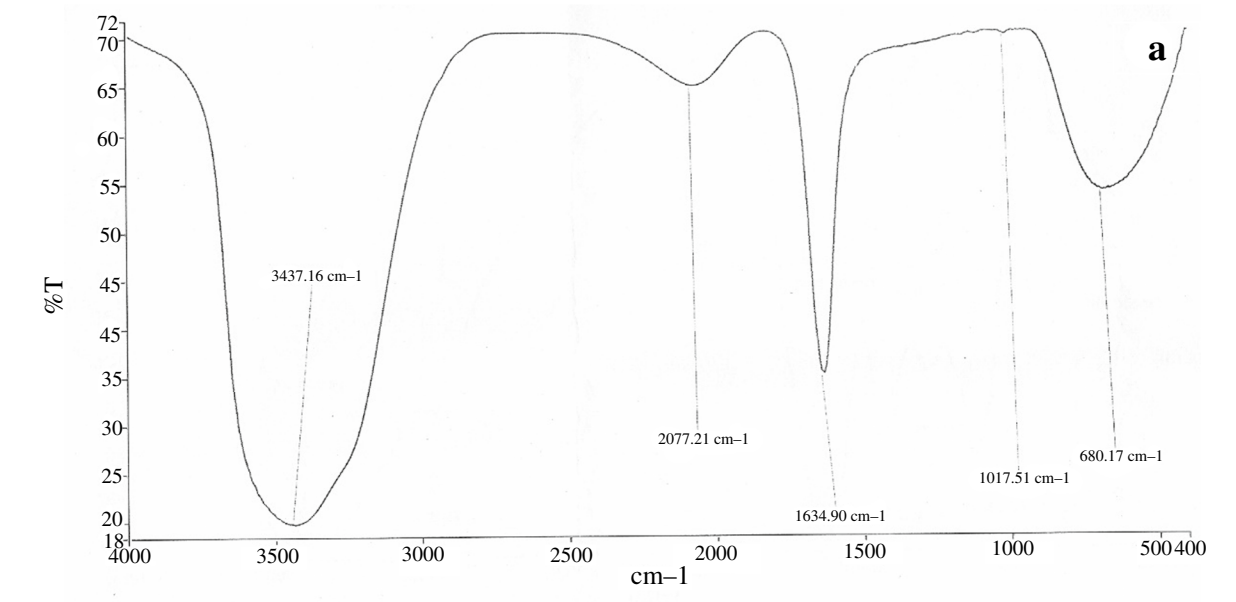

FTIR spectrum of aqueous leaf extract of *Diospyros montana*

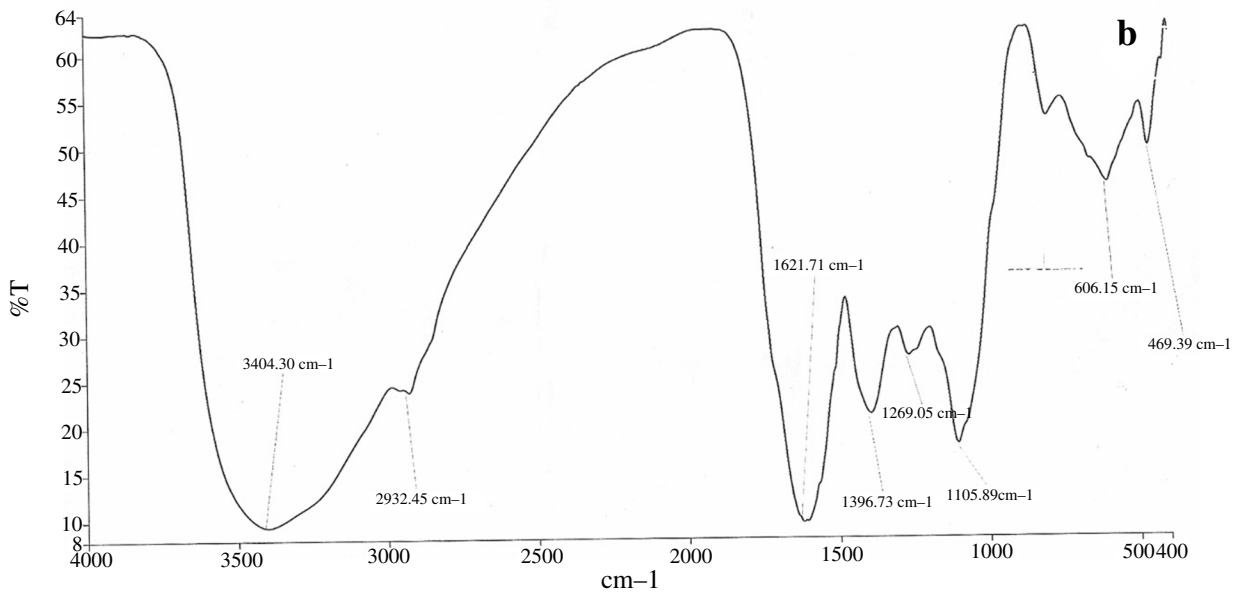

FTIR spectrum of CuO-NPs synthesized from *Diospyros montana* leaf extract

Fig. 5 A FTIR spectrum of aqueous leaf extract of *Diospyros montana*. B FTIR spectrum of CuO-NPs synthesized from *Diospyros montana* leaf extract

of NPs reconstituted in dimethyl sulphoxide (DMSO). All the plates were incubated at 37^0C for 24 h.

Zone of inhibition against the test microorganisms was measured with antibiotic Zone Scale (PW297, Himedia Labs Pvt. Ltd., Mumbai, India), which was held over the back of inverted plate. Each petri plate was held a few inches above a black, non-reflecting background and illuminated with reflected light. DMSO was used as negative

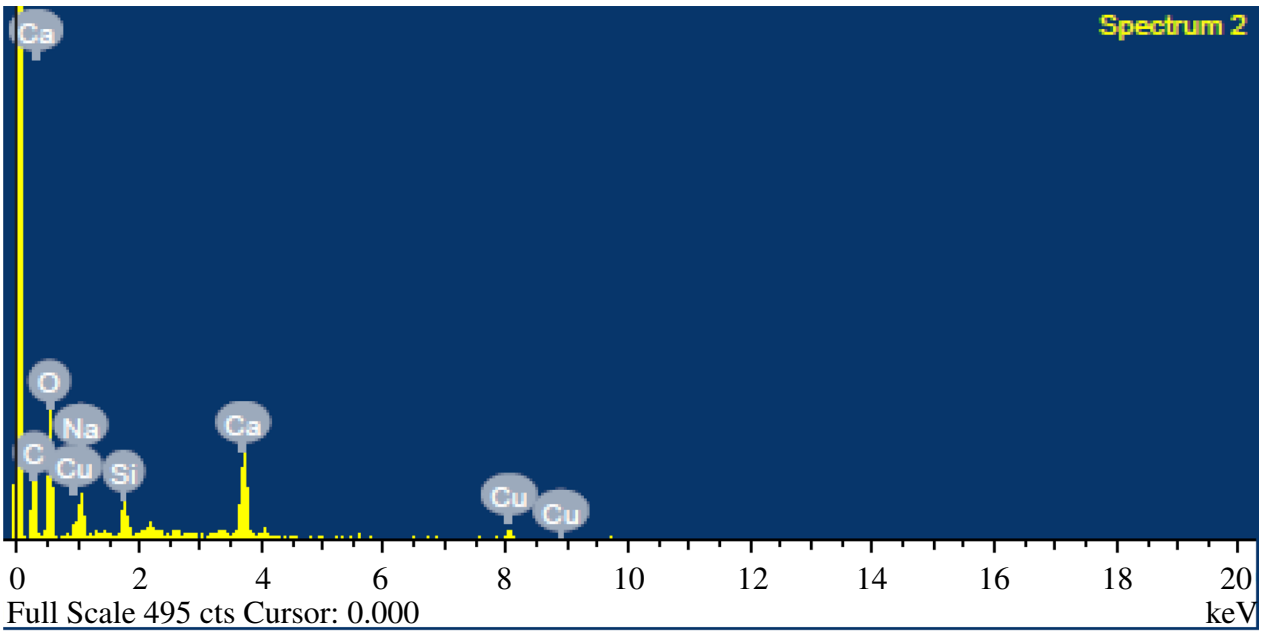

Quantitative results

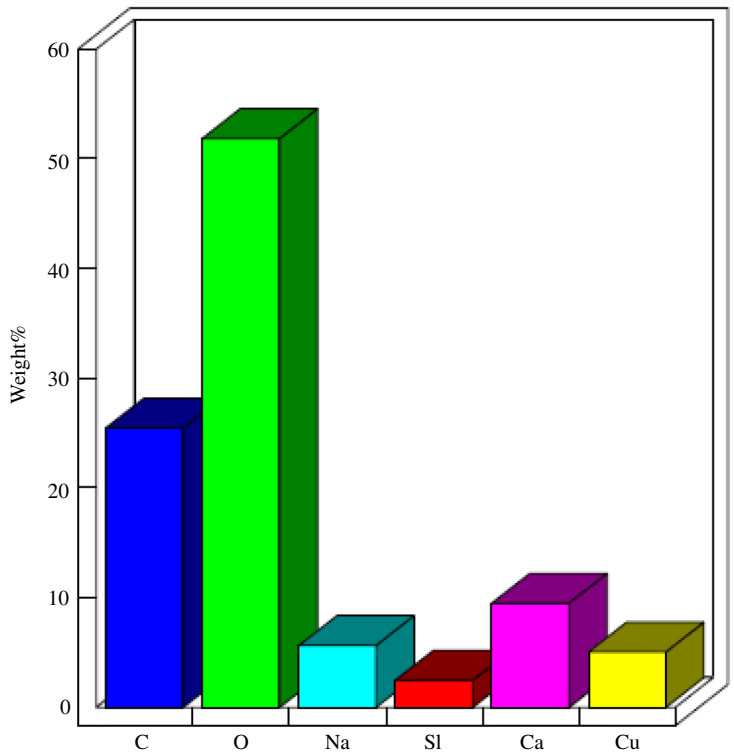

Element	Weight%	Atomic%
C K	27.21	36.99
O K	52.14	53.20
Na K	3.74	2.66
Si K	4.86	2.82
Ca K	8.21	3.34
Cu K	3.84	0.99
Totals	100.00	

Fig. 6 EDX profile of CuO-NPs

control, whereas media with norfloxacin (5 µg/disk, standard antibiotic for Gram-positive bacteria) and gentamicin (10 µg/disk, standard antibiotic for Gram-negative bacteria) were used as positive control. In order to eliminate error, all experiments were done in triplicate and the p value was calculated using Microsoft Excel program.

Distribution Results

	Mode ± SD (nm)	%Pd	Est. MW (KDa) (Mode ± SD)*	% Intensity	% Mass	Peak Polydispersity
Peak 1:	82.09 ± 20.32	24.9	1.01e+5 ± 3.94e+4	8.2	0.5	Polydisperse
Peak 2:	477.7 ± 192.0	39.2	6.25e+6 ± 8.33e+5	76.6	24.2	Polydisperse
Peak 3:	2780 ± 311.7	12.5	3.85e+8 ± 7.38e+7	15.2	75.3	Monodisperse

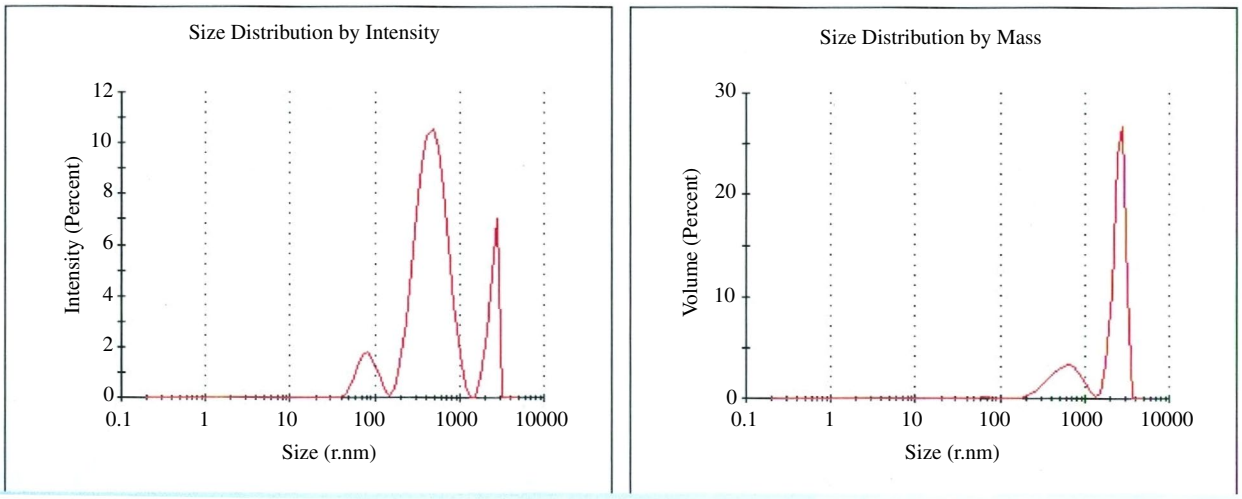

Fig. 7 Particle size distribution

Results

HPLC and UV–Vis spectroscopy

The HPLC profile of the aqueous leaf extract of *D. montana* shows 6 peaks at 273 nm and 8 peaks at 252 nm. At 273 nm, peak number 5 at 3.225 retention time and at 252 nm, peak no. 8 at retention time 3.745 are the peaks with maximum concentration in the injected sample, respectively. The results are shown in Fig. 1 and Table 1. UV–Vis spectrum of aqueous leaf extract of *D. montana* absorbs at 273 nm (Fig. 2). When leaf extract is added to $CuSO_4$ solution its color starts to change from light blue to yellowish and eventually turns black after 20 min. However, on heating this mixture the reaction proceeds vigorously and completes within 5 min, but the particle size becomes larger perhaps owing to their agglomeration. Formation of CuO-NPs was monitored by UV–Vis spectrum which showed a broad peak at 320 nm (Fig. 3). We have run the UV–Vis spectrum of $CuSO_4$ solution also in order to distinguish between the CuO-NPs and any excess of $CuSO_4$ or leaf extract of *D. montana*. However, $CuSO_4$ did not exhibit any peak in the ultra-violet region, but showed a very sharp broad signal at 809.5 nm in visible range due to d → d charge transfer (Fig. 4).

IR spectra

Although several phytochemicals have been detected in *D. montana*, diospyrin is the main constituent of the extract which is also evidenced from its FTIR spectrum (Fig. 5a, b). The present spectrum of extract shows a very prominent peak at 1635 cm^{-1} owing to double quinonoid structure of diospyrin which has been assigned to C=O stretching frequency [26]. The peak appearing at 3437 cm^{-1} has been assigned to ν(O–H) of water molecules. IR spectrum of CuO-NPs synthesized from leaf extract of *D. montana* exhibits a slight shift in carbonyl stretching frequency from 1635 to 1621 cm^{-1} after the formation of NPs. It is the characteristic frequency of diospyrin which distinguishes it from other molecules containing only one quinonoid group because of their different range of ν(C=O). It indicates that only C=O group of diospyrin takes part in the transformation of copper sulfate to copper oxide NPs. Since Cu–O bond in CuO NPs is very strong the Cu–O stretching vibration appears in the lower region of IR spectrum. It becomes important when copper is coordinated to an electron donating species. However, we have not observed any new peak in the FTIR spectrum of CuO-NPs, we therefore rule out the coordination of copper ion to any other donor group.

EDX analysis

The energy dispersive X-ray (EDX) spectroscopy of CuO-NPs (Fig. 6) detects both qualitatively and quantitatively the elements present in the sample. The profile shows

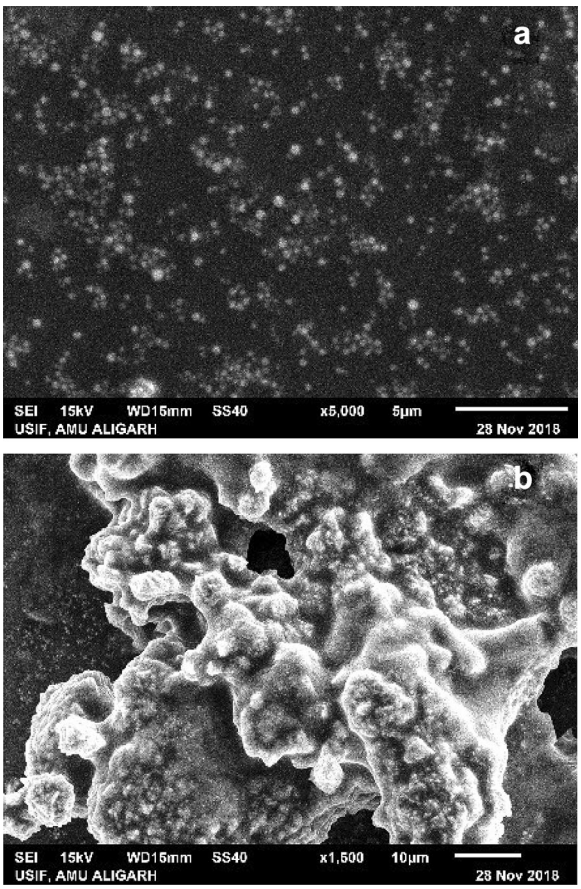

Fig. 8 SEM images of CuO-NPs taken at different magnification**s a** 5 μm and **b** 10 μm

the presence of Cu, Ca, C, O, Na, Si and oxygen in varying percentages. Three signals appear for Cu at 1, 8 and 9 keV. The calculated value of copper and oxygen in CuO comes out to be 79.88% and 20.11%, respectively. EDX analysis shows small quantity of copper (3.8%) and fairly large quantity of oxygen (52.1%).

Size distribution

Size distribution study was done with dynamic light scattering (DLS) technique at 25 °C at 357.8 derived count rate (K cps). Water was used as solvent. The NPs were 70% polydispersed with an estimated molecular weight of 6.79 ± 4.75. The spectrum displays 3 peaks corresponding to three types of CuO-NPs. CuO-NPs of 477 ± 192 nm are in abundance and constitute 76.6% by intensity (Fig. 7). Mass distribution showed that largest and heaviest particles (Peak 3) constitute only 15.2% of the total NPs and they are monodispersed while all other NPs are polydispersed.

SEM, TEM and SAED analysis

SEM micrograph shows morphology of CuO-NPs. SEM images at high resolution show well-dispersed CuO-NPs of different sizes even though all of them are spherical in shape. Size and shape vary with method of fabrication and nature of reducing chemicals. For instance, a weak acid like oxalic acid, citric acid and ascorbic acids are weak reducing agent while alcohol, phenol and amines are strong reducing agents and give good yield. CuO-NPs appear to be scattered. At 25,000 magnification they appear like pearls studded in the sky (Fig. 8). TEM (Fig. 9) and SEM images are very similar showing spherical NPs. The selected area electron diffraction (SAED) displays a circular ring which is the characteristic of crystalline nature of NPs (Fig. 10). The figure shows stacking of NPs in groups. They appear to be aggregated and connected to each other. The physical appearance of CuO-NPs is also spherical.

Photocatalytic degradation

Photocatalytic activity of CuO-NPs has been studied at room temperature in the daylight. Ten ml of 20 ppm solution of MB dye in presence of 0.1 g ascorbic acid as reducing agent and about 1–2 mg of CuO as catalyst were taken together in a closed vessel and stirred well. Photodegradation of the dye started immediately and took 90 s to complete the reduction process which was reflected from the disappearance of the blue color of the dye. The degradation in presence of ascorbic acid alone takes 10 min.

Antibacterial activity

In vitro antibacterial activity of CuO-NPs against seven Gram-positive (*S. aureus, S. mutans, B. cereus, S. pyogenes, S. viridans, S. epidermidis* and *C. xerosis*) and four Gram-negative bacterial strains (*E. coli, K. pneumoniae, P. vulgaris, and P. aeruginosa*) has been screened and the results are presented in Table 2 and Fig. 11.

Discussion

In the present study, we fabricated the CuO-NPs of 5.9 to 21.8 nm via green route, which has received more attention because of the eco-friendly and cost-effective approach [10]. Biogenic fabrication of NPs from plant material has been reported earlier, where various phytochemicals, ranging from primary metabolites to low molecular weight secondary metabolites, for instance terpenoids, alkaloids, polyphenols, quinones, etc., have been reported [30, 31].

Aqueous leaf extract of *D. montana* absorbs at 273 nm in the UV–Vis region of the spectrum. This absorption in the lower region is mainly due to phenolic ring system

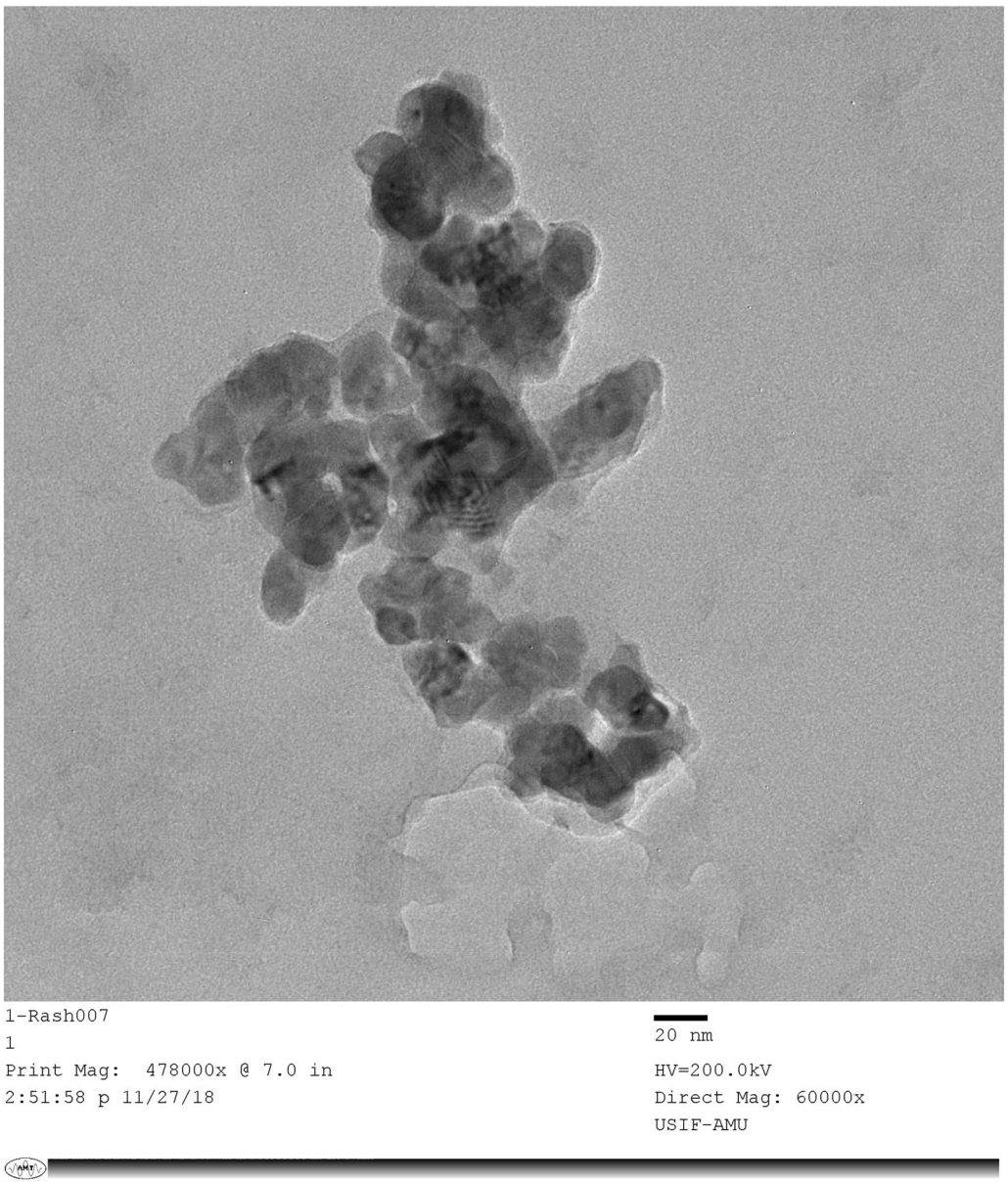

Fig. 9 TEM of CuO-NPs

which is alluded to the $\pi \rightarrow \pi^*$ transition. It depends on the type of the phytochemicals available in the plant extract. Further, formation of CuO-NPs showed a broad peak at 320 nm as a consequence of their surface plasmon resonance (SPR) and the shape of NPs [32]. It is the characteristic peak of black cupric oxide NPs the intensity of which depends on their concentration and aggregation. Aggregation of NPs does not occur at lower concentration and hence the absorption peak is very sharp. SPR generally varies with dispersion medium and the dispersed phase. Also, the color of the dispersed phase depends on the size, shape and charge on the NPs. Since they are highly stable, their spectrum does not show any significant variation even after several days.

Although, several phytochemicals have been detected in *D. Montana* [28, 33], diospyrin is the main constituent which is also demonstrated from the FTIR spectral studies. As reported earlier [29], the present spectrum of extract shows a peak at 1635 cm^{-1} due to double quinonoid structure of diospyrin which has been assigned to C=O stretching frequency [34]. The CuO-NPs shows a slight shift in carbonyl stretching frequency from

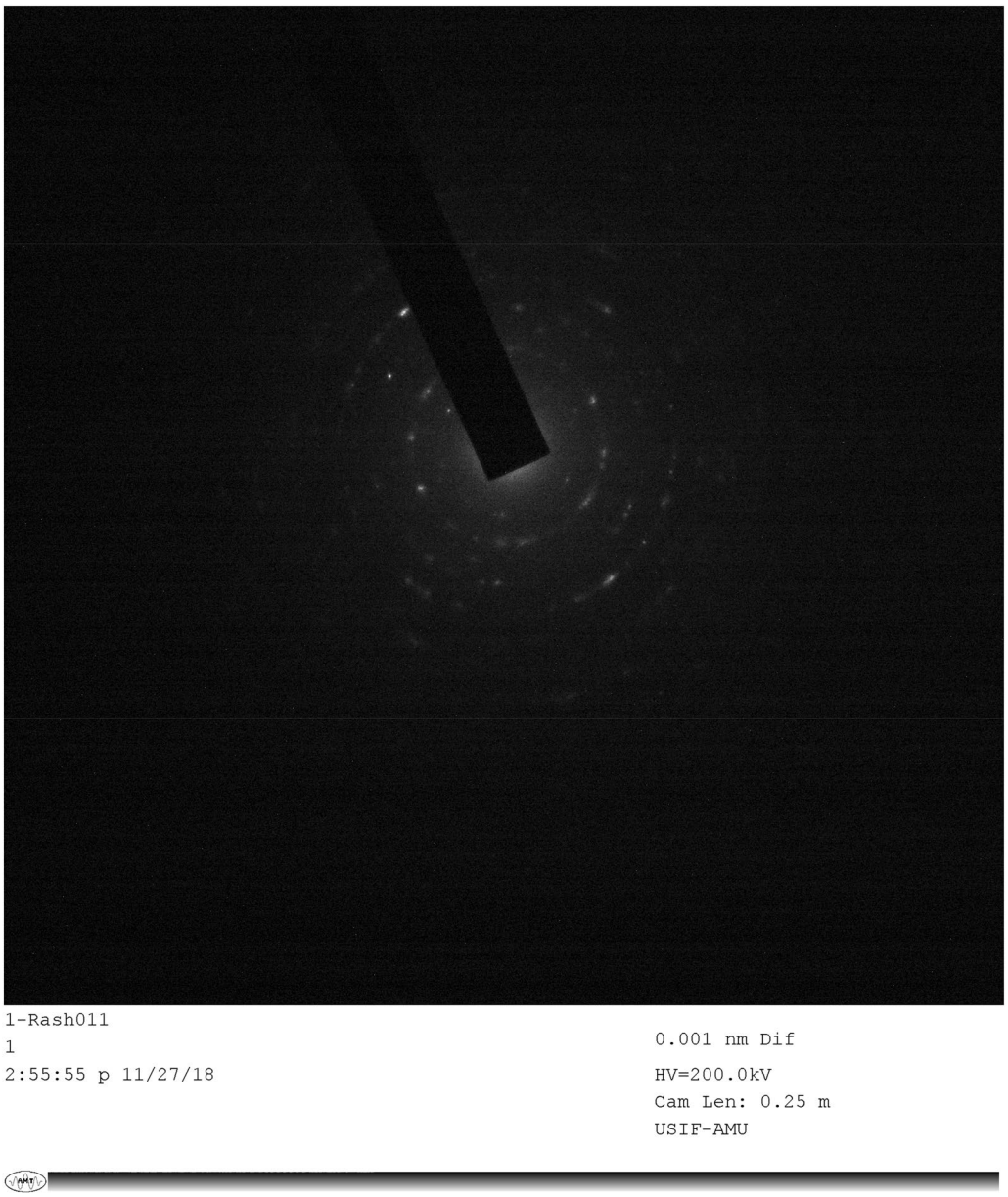

Fig. 10 SAED image of CuO-NPs

1635 cm^{-1} to 1621 cm^{-1} after NPs formation. It is the characteristic frequency of diospyrin which distinguishes it from other molecules containing only one quinonoid group because of their different range of ν(C=O). It indicates that only C=O group of diospyrin takes part in the transformation of copper sulfate to copper oxide NPs. Since Cu–O bond in CuO-NPs is very strong the Cu–O stretching vibration appears in the lower region of IR spectrum. It becomes important when copper is coordinated to an electron donating species. However, we have not observed any new peak in the FTIR spectrum of CuO-NPs, therefore, we rule out the coordination of copper ion to any other donor group. The peak appearing at 4337 cm^{-1} has been assigned to ν(O–H) of water molecules.

The EDX shows the presence of Cu, Ca, C, O, Na and Si in varying percentages. Elements other than copper and oxygen are mainly due to impurity in the glassware which would have come during washing and sample preparation. They may influence the CuO morphology,

Table 2 Mean zone of inhibition (in mm) of CuO-NPs against bacterial strains

Bacterial strains	CuO-NPs	Negative control (NC)[a]	Positive control (PC)[b]
Staphylococcus aureus	20.33 ± 0.88 (1.52) S	6.66 ± 0.33 (0.57) R	10.66 ± 0.33 (0.57) S
Streptococcus mutans	17.66 ± 0.88 (1.52) S	6.33 ± 0.33 (0.57) R	14.66 ± 0.33 (0.57) S
Streptococcus pyogenes	18.66 ± 0.33 (0.57) S	6.33 ± 0.33 (0.57) R	14.33 ± 0.33 (0.57) S
Streptococcus viridans	15.33 ± 0.33 (0.57) S	6.33 ± 0.33 (0.57) R	12.33 ± 0.33 (0.57) S
Staphylococcus epidermidis	7.33 ± 0.33 (0.57) S	6.33 ± 0.33 (0.57) R	10.33 ± 0.33 (0.57) S
Corynebacterium xerosis	17.33 ± 0.33 (0.57) S	6.33 ± 0.33 (0.57) R	12.33 ± 0.33 (0.57) S
Bacillus cereus	18.66 ± 0.33 (0.57)	6.33 ± 0.33 (0.57) R	12.33 ± 0.66 (1.15) S
Escherichia coli	13.33 ± 0.33 (0.57) S	6.33 ± 0.33 (0.57) R	18.33 ± 0.33 (0.57) S
Klebsiella pneumoniae	20.33 ± 0.33 (0.57) S	6.33 ± 0.33 (0.57) R	28.33 ± 0.33 (0.57) S
Pseudomonas aeruginosa	17.33 ± 0.33 (0.57) S	6.33 ± 0.33 (0.57) R	14.33 ± 0.33 (0.57) S
Proteus vulgaris	11.33 ± 0.33 (0.57) S	6.33 ± 0.33 (0.57) R	22.33 ± 0.33 (0.57) S

Values are expressed as mean ± SE; where, S = sensitive (> 7 mm zone of inhibition), R = resistant (< 7 mm zone of inhibition), [a]Dimethyl sulphoxide, [b]Standard drug norfloxacin for Gram-positive and gentamicin for Gram-negative strains)

but catalytic and antimicrobial properties of CuO-NPs are not affected. Three signals appear for copper at 1, 8 and 9 keV. Although, the calculated value of copper and oxygen in CuO comes out to be 79.88% and 20.11%, respectively, EDX analysis shows small quantity of copper (3.8%) and substantial quantity of oxygen (52.1%). It is quite obvious that atmospheric oxygen is associated with other elements as impurity. NPs are 69.9% polydispersed with an estimated molecular weight of 6.79 ± 4.75. Their average e hydrodynamic radius is 495.0 ± 346.3 due to hydration of CuO-NPs because of high affinity of copper for oxygen. The hydrodynamic radii always increase with decreasing size of NPs. The CuO-NPs are in abundance and constitute 76.6% by intensity. However, distribution by mass shows that the largest and heaviest particles are only 15.2% and monodispersed, while all other NPs are polydispersed. The polydispersity index (0.489) well below 0.7 shows excellent quality of the CuO NPs [32] even though they are contaminated with other elements too. CuO-NPs were spherical shaped. Size and shape vary with method of fabrication and nature of reducing chemicals. For instance, a weak acid like oxalic acid, citric acid and ascorbic acids are weak reducing agents while alcohol, phenol and amines are strong reducing agents and give good yield. They were crystalline in nature.

Reduction of MB by ascorbic acid as reducing agent in presence of CuO-NPs as catalyst has been achieved in 90 s at room temperature while the reduction of the dye by ascorbic acid alone takes more than 10 min. It is noteworthy that when the reduced form of the dye is shaken, it turns blue again even after 2 months. However, on standing for 2 min it is decolorized again. The color disappears when electrons move from valence band to conduction band, but when it absorbs energy from sunlight it turns blue again. It is a cyclic process which is very efficient and can be used to recover either the original MB or its reduced form. However, CuO-NPs can be used as an efficient catalyst in the photodegradation of dyes. It is known that the MB is an aromatic cationic dye, and extensively used in textile industries for various purposes.

It is clear from the zone of inhibition that all the values are significant. Further, the toxic effect of NPs on Gram-positive bacteria is relatively higher than those for Gram-negative strains. It is quite obvious that CuO-NPs may be effectively used against Gram-positive bacteria in vitro to prevent their replication. It is visible from the zone of inhibition that CuO-NPs are more toxic to all Gram-positive bacteria than even the standard drug norfloxacin. The toxicity of CuO-NPs against various bacteria follows the order:

S. aureus > *S. pyogenes* = *B. cereus* > *S. mutans* > *C. xerosis* > S. *viridans* > S. *epidermidis*.

The CuO-NPs are significantly toxic to both Gram-positive and Gram-negative pathogenic bacterial strains studied under this project. The nanoparticles inhibit the growth of microbes by penetrating in the body leading to their death. Deposition of NPs in the bacterial cell has been confirmed from the EDX analysis of bacteria treated with CuO-NPs [35]. The NPs get accumulated in the microbial cell which swells due to increased volume and eventually bursts.

Since the other hypothesis of CuO-NPs inhibiting the bacterial cell multiplication by releasing copper ions and then disrupting vital metabolic functions by binding with the nitrogen atoms of amino acids through lone pair of electrons has not been supported by experimental evidences, it is less reliable (13, 36).

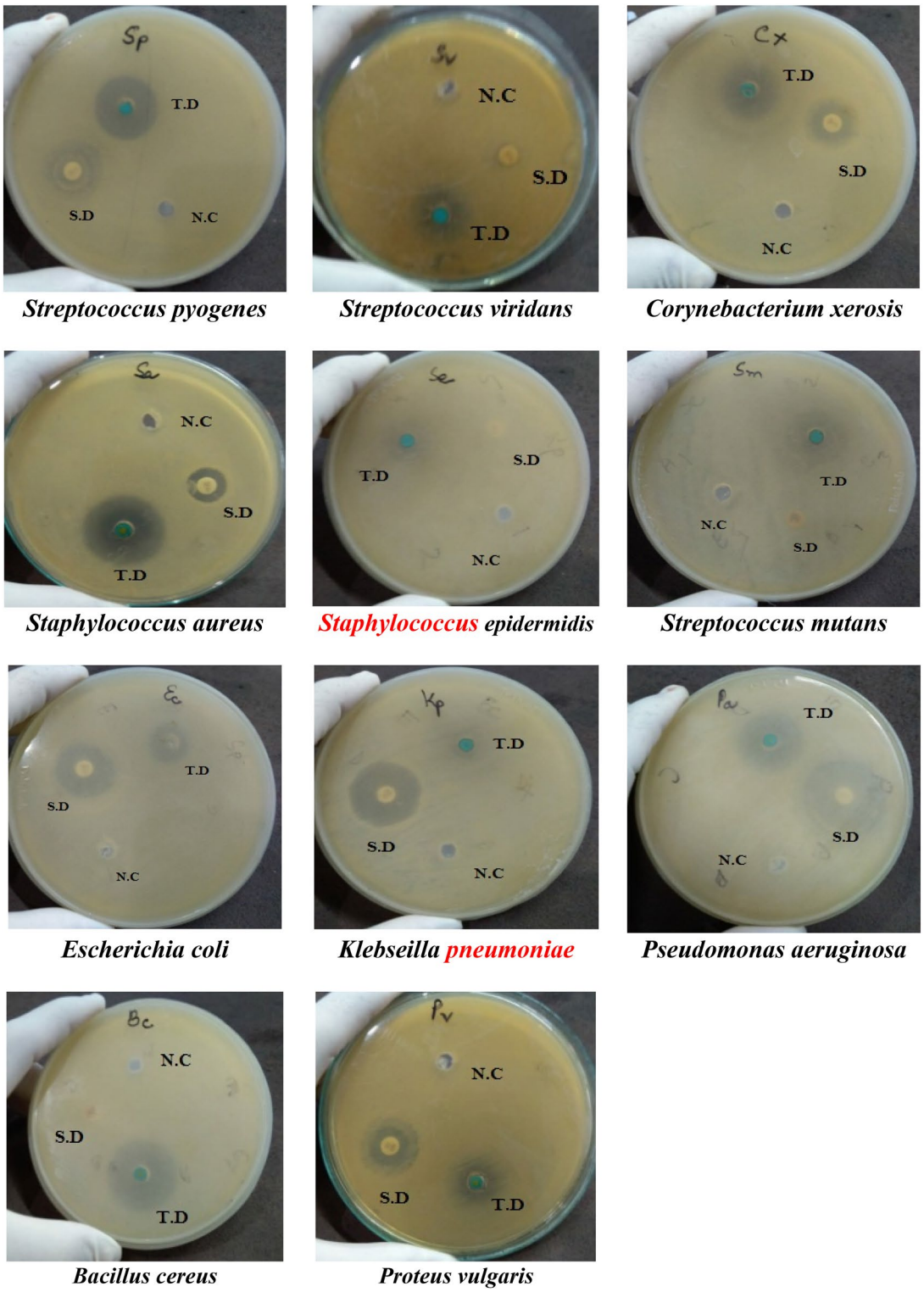

Fig. 11 Antibacterial activity of CuO-NPs against selected Gram-negative and Gram-positive bacteria in a nutrient agar medium depicting zones of inhibition (where T.D. = test drug; S.D. = standard drug; and N.C. = negative control)

Conclusion

CuO-NPs of 5.9–21.8 nm have been fabricated from *D. montana* leaf extract in aqueous medium at ambient temperature. It is inexpensive and easy to fabricate from plant materials without using any organic solvent. Since CuO-NPs are toxic to both Gram-positive and Gram-negative bacteria they can be exploited to inhibit the multiplication of pathogens. Attempt may be made to use them as antibacterial agent to protect food, vegetable and crops. Since the green synthesized CuO-NPs showed efficient photocatalytic degradation of methylene blue, they can be used as catalyst in the reduction of dyes, other toxic material and industrial effluents.

Abbreviations

NPs: Nanoparticles; CuO-NPs: Cupric oxide nanoparticles; UV–Vis: Ultraviolet–visible spectroscopy; SEM: Scanning electron microscopy; TEM: Transmission electron microscopy; XRD: X-ray diffraction; FTIR: Fourier transform infrared spectroscopy; SAED: Selected area (electron) diffraction; EDX: Energy-dispersive X-ray spectroscopy; MB: Methylene blue.

Acknowledgements

We acknowledge with thanks the assistance provided by the University Sophisticated Instrument Facility (USIF) and the Department of Microbiology, Jawaharlal Nehru Medical College & Hospital, Aligarh Muslim University, Aligarh, India, for providing bacterial culture.

Authors' contributions

KSS and AH conceived the experiments and research plans; MR, AR, T and SR performed most of the experiments; KSS supervised the experiments; KSS and AH analyzed the data and wrote this paper. All authors read and approved the final manuscript.

Funding

Not applicable.

Availability of data and materials

The data sets supporting the results of this work are included in the article.

Ethics approval and consent to participate

Not applicable.

Consent for publication

Not applicable.

Competing interests

The author(s) declared no potential conflicts of interest with respect to the research, authorship, and/or publication of this article.

Author details

[1] Department of Chemistry, Aligarh Muslim University, Aligarh 202002, Uttar Pradesh, India. [2] Department of Saidla, Aligarh Muslim University, Aligarh 202002, Uttar Pradesh, India. [3] Wolaita Sodo University, P.O. Box: 138, Wolaita, Ethiopia. [4] Department of IlmulAdvia, Aligarh Muslim University, Aligarh 202002, Uttar Pradesh, India.

Received: 19 May 2020 Revised: 24 September 2020 Accepted: 29 September 2020
Published online: 23 December 2020

References

1. Pileni MP, Lisiecki I. Nanometer metallic copper particle synthesis in reverse micelles. Colloids Surf A. 1993;80:63–8.
2. Siwach OP, Sen P. Synthesis and study of fluorescence properties of Cu nanoparticles. J Nanopart Res. 2008;10:107–14.
3. Singh M, Sinha I, Premkumar M, Singh AK, Mandal RK. Structural and surface plasmon behavior of Cu nanoparticles using different stabilizers. Colloid Surf A. 2019;359:88–94.
4. Vazquez-Vazquez C, Banobre-Lopez M, Mitra A, Arturo Lopez-Quintela M, Rivas J. Synthesis of small atomic copper clusters in microemulsions. Langmuir. 2009;25:8208–16.
5. Husen A, Siddiqi KS. Plants and microbes assisted selenium nanoparticles: characterization and application. J Nanobiotechnol. 2014a;12:28.
6. Husen A. Natural product-based fabrication of zinc-oxide nanoparticles and their applications. In: Husen A, Iqbal M, editors. Nanomaterials and plant potential. Cham: Springer International Publishing; 2019. p. 193–291.
7. Siddiqi KS, Husen A. Fabrication of metal and metal oxide nanoparticles by algae and their toxic effects. Nano Res Lett. 2016a;11:363.
8. Siddiqi KS, Husen A. Fabrication of metal nanoparticles from fungi and metal salts: scope and application. Nano Res Lett. 2016b;11:98.
9. Sastry ABS, Aamanchi RBK, Prasad CSRL, Murty BS. Large-scale green synthesis of Cu nanoparticles. Environ Chem Lett. 2013;11:183–7.
10. Husen A, Siddiqi KS. Phytosynthesis of nanoparticles: concept, controversy and application. Nano Res Lett. 2014b;9:229.
11. Siddiqi KS, Husen A, Rao RAK. A review on biosynthesis of silver nanoparticles and their biocidal properties. J Nanobiotechnol. 2018;16:14.
12. Sankar R, Manikandan P, Malarvizhi V, Fathima T, Shivashangari KS, Ravikumar V. Green synthesis of colloidal copper oxide nanoparticles using *Carica papaya* and its application in photocatalytic dye degradation. Spectrochim Acta A Mol Biomol Spectrosc. 2014;121:746–50.
13. Arunachalam R, Dhanasingh S, Kalimuthu B, Uthirappan M, Rose C, Mandal AB. Phytosynthesis of silver nanoparticles using *Coccinia grandis* leaf extract and its application in the photocatalytic degradation. Colloids Surf B Biointerfaces. 2012;94:226–30.
14. Kumar P, Govindaraju M, Senthamilselvi S, Premkumar K. Photocatalytic degradation of methyl orange dye using silver (Ag) nanoparticles synthesized from *Ulva lactuca*. Colloids Surf B Biointerfaces. 2012;103:658–61.
15. Zheng XG, Xu CN, Tomokiyo Y, Tanaka E, Yamada H, Soejima Y. Observation of charge stripes in cupric oxide. Phys Rev Lett. 2000;85:5170–3.
16. Srivastava A. Antiviral activity of copper complexes of isoniazid against RNA tumor viruses. Resonance. 2009;14:754–60.
17. Santo CE, Quaranta D, Grass G. Antimicrobial metallic copper surfaces kill *Staphylococcus haemolyticus* via membrane damage. Microbiology Open. 2012;1:46–52.
18. Grass G, Rensing C, Solioz M. Metallic copper as an antimicrobial surface. Appl Environ Microbiol. 2011;77:1541–7.
19. Nadkarni KM. Indian materia medica. Bombay: Popular Prakashan Pvt. Ltd.; 1976. p. 48.
20. Nasrollahzadeh M, Maham M, Sajadi SM. Green synthesis of CuO nanoparticles by aqueous extract of *Gundelia tournefortii* and evaluation of their catalytic activity for the synthesis of N-monosubstituted ureas and reduction of 4-nitrophenol. J Colloid Interface Sci. 2015;455:245–53.
21. Adzet T, Puigmacia M. High-performance liquid chromatography of caffeoylquinic acid derivatives of Cynara scolymus L. leaves. J Chromatography. 1985;A348:447–53.
22. Haghi G, Hatami A, Arshi R. Distribution of caffeic acid derivatives in *Gundelia tournefortii* L. Food Chem. 2011;124:1029–35.
23. Nagajyothi PC, Muthuraman P, Sreekanth TVM, Kim DH, Shim J. Green synthesis: In-vitro anticancer activity of copper oxide nanoparticles against human cervical carcinoma cells. Arab J Chem. 2017;10:215–25.
24. Nasrollahzadeh M, Maham M, Rostami-Vartooni A, Bagherzadeh M, Sajadi SM. Barberry fruit extract assisted in situ green synthesis of cu nanoparticles supported on a reduced graphene oxide–Fe_3O_4 nanocomposite

as a magnetically separable and reusable catalyst for the O-arylation of phenols with aryl halides under ligand-free conditions. RSC Adv. 2015;5:64769–80.
25. Nasrollahzadeh M, Mohammad Sajadi S, Rostami-Vartooni A. Green synthesis of CuO nanoparticles by aqueous extract of *Anthemis nobilis* flowers and their catalytic activity for the A^3 coupling reaction. J Colloid Interface Sci. 2015;459:183–8.
26. Pietta PG, Mauri PL, Manera E, Ceva PL, Rava A. An improved HPLC determination of flavonoids in medicinal plant extracts. Chromatographia. 1989;27:509–12.
27. Nasrollahzadeh M, Sajadi SM, Rostami-Vartooni A, Bagherzadeh M. Green synthesis of Pd/CuO nanoparticles by Theobroma cacao L seeds extract and their catalytic performance for the reduction of 4-nitrophenol and phosphine-free Heck coupling reaction under aerobic conditions. J Colloid Interface Sci. 2015;448:106–13.
28. Anonymous, The wealth of India, first supplement series. CSIR- national institute of science communication and informative resources. Dr K.S. Krishanan Marg, New Delhi Vol. 3: D-I, 2013, pp. 28.
29. Siddiqi KS, Tajuddin RM, Rehman S, Husen A. Synthesis of silver nanoparticles using aqueous leaf extract of *Diospyros montana* Roxb. and their antimicrobial activity against some clinical isolates. Bio Nano Sci. 2019;9:302–12.
30. Bachheti RK, Fikadu A, Bachheti A, Husen A. Biogenic fabrication of nanomaterials from flower-based chemical compounds, characterization and their various applications: a review. Saudi J Biol Sci. 2020;27:2551–62.
31. Siddiqi KS, Husen A. Current status of plant metabolite-based fabrication of copper/copper oxide nanoparticles and their applications: A review. Biomat Res. 2020;24:11.
32. Zhang JZ, Nogues C. Plasmonic optical properties and application of metal nanostructures. Plasmonics. 2008;3:127–50.
33. Sharma V. *Diospyros Montana* Roxb.: a source of 1,4-naphthoquinone dimers counting diospyrin esters. IOSR J Appd Chem. 2017;10:25–6.
34. Bellamy LJ. The infra-red spectra of complex molecules, vol. 1 3rd edn. Dordrecht: Springer; 1975. p. 433.
35. Vaidehi D, Bhuvaneshwari V, Bharathi D, Sheetal BP. Antibacterial and photocatalytic activity of copper oxide nanoparticles synthesized using *Solanum lycopersicum* leaf extract. Mater Res Express. 2018;5:085403.
36. Balakumaran MD, Ramachandran R, Balashanmugam P, Mukeshkumar DJ, Kalaichelvan PT. Mycosynthesis of silver and gold nanoparticles: Optimization, characterization and antimicrobial activity against human pathogens. Microbiol Res. 2016;182:8–20.

Publisher's Note